

# MgZnO metal–semiconductor–metal structured solar-blind photodetector with fast response

L.K. Wang<sup>a,b</sup>, Z.G. Ju<sup>a,b</sup>, C.X. Shan<sup>a</sup>, J. Zheng<sup>a,b</sup>, D.Z. Shen<sup>a</sup>, B. Yao<sup>a</sup>, D.X. Zhao<sup>a</sup>, Z.Z. Zhang<sup>a</sup>, B.H. Li<sup>a</sup>, J.Y. Zhang<sup>a,\*</sup>

<sup>a</sup> Key Laboratory of Excited State Processes, Changchun Institute of Optics, Fine Mechanics and Physics, Chinese Academy of Sciences, No.3888 East South-Lake Road, Changchun 130033, People's Republic of China

<sup>b</sup> Graduate School of the Chinese Academy of Sciences, Beijing 100039, People's Republic of China

## ARTICLE INFO

### Article history:

Received 15 July 2009

Received in revised form

6 August 2009

Accepted 21 August 2009 by P. Sheng

Available online 29 August 2009

### PACS:

73.40.Sx

72.40.+w

81.15.Gh

### Keywords:

A. Semiconductors

B. MOCVD

C. Metal–semiconductor–metal

C. Fast response

## ABSTRACT

A  $\text{Mg}_{0.48}\text{Zn}_{0.52}\text{O}$  thin film was deposited on a sapphire substrate by metal-organic chemical vapor deposition, and the thin film exhibits a single cubic phase with high crystal quality from X-ray diffraction measurements. A metal–semiconductor–metal (MSM) structured photodetector was fabricated on the film. The device exhibits a peak response of 268 nm with a cutoff wavelength at 283 nm. Rise and decay times of 10 ns and 150 ns, respectively, are obtained with a load resistance of 50  $\Omega$ . The pulse response for the device is limited by the RC time constant.

© 2009 Elsevier Ltd. All rights reserved.

## 1. Introduction

Solar-blind photodetectors are of great importance for their versatile applications in missile warning and tracking, engine/flame monitoring, chemical/biological agent detection, secure intersatellite communications, and underwater/sub-marine communication systems, etc [1–3]. Recently, wide band gap semiconducting materials, including GaN and ZnO, have received much attention due to their high sensitivity in ultraviolet detection, and some progress milestones have been achieved in the preparation of solar blind photodetectors based on these materials [4–8]. Compared with Schottky and pin structures, metal–semiconductor–metal (MSM) photodetectors are an attractive choice for solar-blind photodetectors considering their simplicity in fabrication processes and suitability for monolithic integration [9]. Especially, the planar structure of MSM structure will lead to an extremely low capacitance, which is eagerly wanted

for large bandwidth and low-noise performance of photodetectors [10]. Biyikli et al. have reported solar-blind AlGaIn MSM photodetectors with response times in the order of the picosecond level [6]. However, the lack of lattice-matched substrates and relatively high defect density limit the further development of AlGaIn based photodetectors [11]. Fortunately, MgZnO possesses unique figures of merit for application in solar-blind photodetectors such as large tunable band gap (3.3–7.8 eV) and low growth temperature (100–750 °C) [12]. In addition, the environmental friendly and biocompatible characteristics make MgZnO alloys more attractive. More recently, our group has reported that a series of MgZnO based photodetectors covered the whole solar blind region [13], which demonstrates the potential of cubic phased MgZnO films in solar blind photodetectors. However, a fast-response MgZnO based solar-blind photodetector has not been reported yet.

In this work, single cubic phased  $\text{Mg}_{0.48}\text{Zn}_{0.52}\text{O}$  thin films were grown by metal-organic chemical vapor deposition (MOCVD), and a MSM structured photodetector was fabricated on the film. A rise and decay time of 10 ns and 150 ns, respectively, is obtained with a load resistance of 50  $\Omega$ .

\* Corresponding author.

E-mail address: [Zhangjy53@yahoo.com.cn](mailto:Zhangjy53@yahoo.com.cn) (J.Y. Zhang).

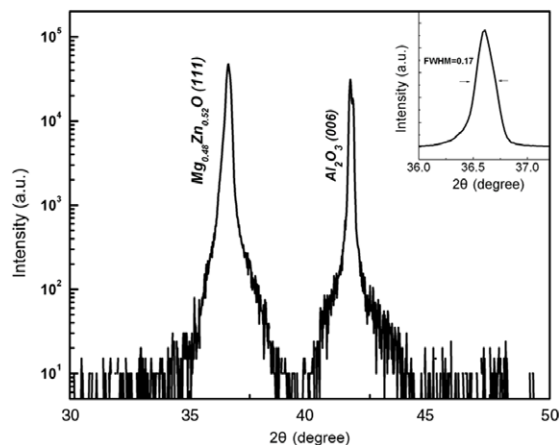


**Fig. 1.** XRD spectrum of the  $\text{Mg}_{0.48}\text{Zn}_{0.52}\text{O}$  thin film. The inset is a magnified profile of the (111) peak.

## 2. Experiment

The  $\text{MgZnO}$  thin film was grown on a sapphire (0001) substrate in a low pressure MOCVD technique. Diethylzinc, biscyclopentadienyl-Mg, and oxygen were employed as precursors, and high purity nitrogen acted as a carrier for the precursors. The deposition temperature was fixed at  $400^\circ\text{C}$  and the pressure at 150 Torr. The composition of the  $\text{MgZnO}$  thin film was measured by a Hitachi S 4800 energy dispersive spectrometer. The structure characterizations were carried out in a Rigaku D/max-RA X-ray diffraction (XRD) employing the  $0.154\text{ nm}$  line of  $\text{Cu K}\alpha$  as the radiation source. The transmission spectra were recorded using a Shimadzu UV-3101PC scanning spectrophotometer. An MSM structured photodetector was fabricated from the  $\text{MgZnO}$  film according to the following procedure: A  $100\text{ nm}$  Au layer was evaporated onto the  $\text{MgZnO}$  film using a vacuum evaporation method. Interdigital Au fingers were obtained through conventional photolithography and wet etching route. The Au fingers were  $500\text{ }\mu\text{m}$  in length and  $5\text{ }\mu\text{m}$  in width, and the interelectrode spacing was  $5\text{ }\mu\text{m}$ . The current–voltage characteristic of the device was measured by a semiconductor parameter analyzer (Keithley 2200). The spectral response of the photodetectors was measured using a  $150\text{ W}$  Xe lamp, monochromator, chopper (EG&G 192), and lock-in amplifier (EG&G 124A). The time resolved response of the photodetector was obtained using a YAG:Nd laser with a wavelength of  $266\text{ nm}$  and a pulse width of  $10\text{ ns}$ .

## 3. Results and discussion

The composition of the film determined by EDX is  $\text{Mg}_{0.48}\text{Zn}_{0.52}\text{O}$ . The structural properties of the  $\text{MgZnO}$  film are shown in Fig. 1. Only one diffraction peak is observed besides the diffraction from the substrate. The peak at  $36.58^\circ$  corresponds to the (111) direction of  $\text{MgZnO}$ . Considering that the diffraction of  $\text{MgO}$  (111) is at  $37.04^\circ$ , the shift towards the small angle side is due to Zn incorporation into  $\text{MgO}$  lattice. The XRD data reveals that the film exhibits a single cubic phase with (111) orientation and no phase separation occurs. According to the phase diagram of the  $\text{ZnO}$ – $\text{MgO}$  system [14], the cubic  $\text{Mg}_x\text{Zn}_{1-x}\text{O}$  films can keep stable in a solid solution state when the Mg content is in the range  $0.55 \leq x \leq 1$  for the cubic phase and  $0 \leq x \leq 0.02$  for the hexagonal phase. And a mixed phase exists when the  $x$  values are outside these two ranges. However, it is known that the solid solubility can be significantly modified in thin film form, and it also depends on the growth conditions. For example, Koike and Yang et al. have demonstrated that the  $\text{MgZnO}$  thin films with a pure hexagonal phase can be obtained with a Mg content of over 30% and 34% by MBE and PLD techniques,

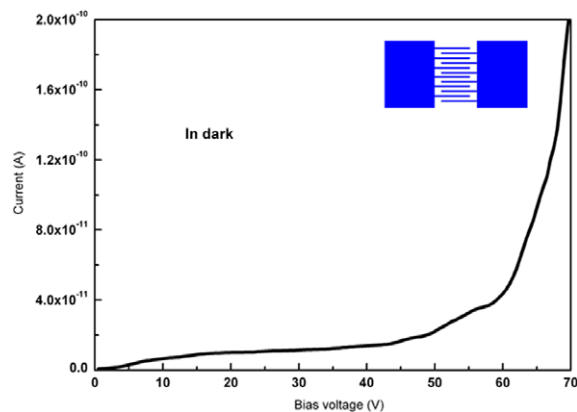


**Fig. 2.**  $I$ – $V$  characteristic of the  $\text{Mg}_{0.48}\text{Zn}_{0.52}\text{O}$  MSM photodetector in dark. The inset is a schematic illustration of the interdigital fingers.

respectively [15,16]. Furthermore, Takeuchi et al. have deposited a single cubic phased  $\text{MgZnO}$  thin film with a Mg content of 50% on a ZnO substrate by the PLD technique [17]. In our case, the relatively low substrate temperature ( $400^\circ\text{C}$ ) makes kinetics instead of thermodynamics dominate the growth process. Thus most radicals do not have enough energy to reach their energy-minimum sites. As a result, single-phased cubic  $\text{Mg}_{0.48}\text{Zn}_{0.52}\text{O}$  film has been obtained. The full width at half maximum (FWHM) of the (111) diffraction peak of the  $\text{Mg}_{0.48}\text{Zn}_{0.52}\text{O}$  film is  $0.17^\circ$ , as shown in the inset of Fig. 1. The narrow width indicates the high crystal quality of the  $\text{Mg}_{0.48}\text{Zn}_{0.52}\text{O}$  film.

A schematic illustration of the interdigital Au electrodes of the  $\text{MgZnO}$  MSM photodetector is shown in the inset of Fig. 2, where the active area of the device is located in the vicinity of the interdigital Au fingers. The typical dark current–voltage ( $I$ – $V$ ) characteristics of the  $\text{MgZnO}$  thin film based MSM photodetectors are shown in Fig. 2. At a bias voltage of  $10\text{ V}$ , the dark current of the photodetector is about  $6.5\text{ pA}$ , which is comparable to the corresponding value ( $10\text{ pA}$  at  $30\text{ V}$  bias) reported in a MSM structured  $\text{AlGaIn}$  solar-blind photodetector [18]. The device exhibits no clear signals of breakdown up to a bias voltage of  $100\text{ V}$ . The low dark current in the MSM detectors was believed to be attributed to the good crystalline quality of the  $\text{MgZnO}$  thin film. Moreover, the nonlinear  $I$ – $V$  characteristic, also found in  $\text{GaIn}$ ,  $\text{AlGaIn}$  MSM photodetectors [6,19], demonstrates the Schottky barrier in the  $\text{MgZnO}$  MSM photodetector.

The spectral response of the  $\text{MgZnO}$  photodetector is present in Fig. 3. The peak photo-response of the device is located at  $268\text{ nm}$  unchanged at different voltages, which is perfectly consistent with the absorption spectrum of the  $\text{MgZnO}$  films (not shown here). The maximum photo response is  $16\text{ mA/W}$  at  $20\text{ V}$  bias and an external quantum efficiency of 7% is achieved for the device. The cutoff wavelength of the photo response is fixed at  $283\text{ nm}$  for the  $\text{MgZnO}$  based MSM photodetector which indicates the solar blind property of the device. A rejection ratio ( $R_{268\text{ nm}}/R_{350\text{ nm}}$ ) of more than 3 orders of magnitude is obtained for the photodetector from the inset, indicating the high long-wavelength rejection power. In addition, a gradual response can also be found in the greater wavelength region, which may result from the composition fluctuations in the  $\text{MgZnO}$  thin film. A similar phenomenon was also found in  $\text{AlGaIn}$  solar blind MSM photodetectors with a high Al content [20].

Fig. 4 shows the pulse response data of the device. The photodetector was connected in series with a load resistor ( $R_L = 50\text{ }\Omega$ ) at a bias voltage of  $30\text{ V}$ . The photo response signal was collected from the device irradiated by the  $266\text{ nm}$  laser pulse. From the figure, the measured pulse response of the  $\text{MgZnO}$  MSM photodetector shows a short rise time and a relatively long fall time. The rise time of the device is  $10\text{ ns}$  which is limited by the

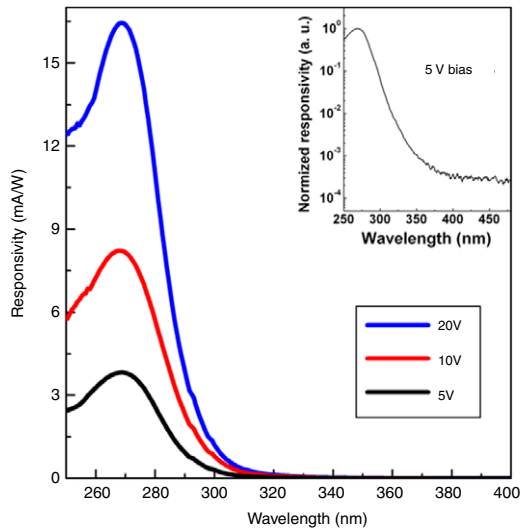


**Fig. 3.** The spectral response of the  $\text{Mg}_{0.48}\text{Zn}_{0.52}\text{O}$  MSM photodetectors at different bias voltage. The inset is a logarithmic response spectrum at 5 V bias.

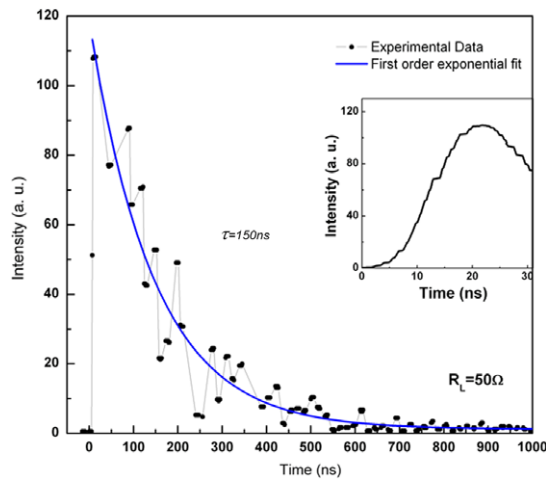


**Fig. 4.** The pulse response of the  $\text{Mg}_{0.48}\text{Zn}_{0.52}\text{O}$  MSM photodetectors and a first order exponential fit of the data. The inset is the detailed rise time of the device pulse response.

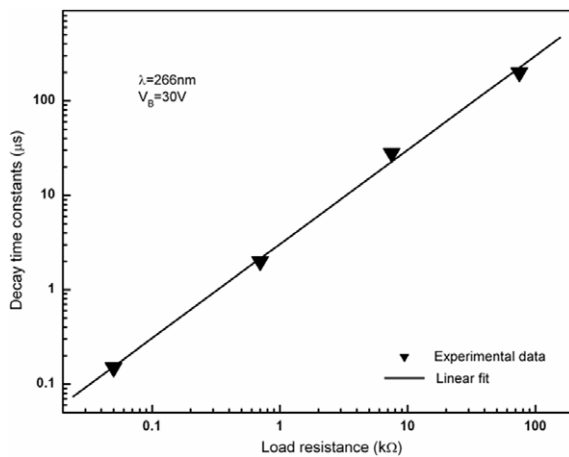


**Fig. 5.** The dependence of decay time on the load resistance for the device.

excitation laser (nominal pulse duration of 10 ns) as shown in the inset. Therefore, the response time of the device is determined by the decay component of the pulse response. In the figure, the experimental data fits well using the exponential curve, where the decay is derived to be 150 ns. This is the first report on the time-

resolved response of solar blind  $\text{MgZnO}$  based photodetectors to the best of the authors' knowledge.

The decay time of the MSM photodetector may be determined by two mechanisms: the carrier transit across the finger gap and the RC time constant, where  $C$  is the sum of the diode internal capacitance and the load capacitance, and  $R$  is the sum of the load resistance ( $R_L$ ) and the series resistance of the device ( $R_S$ ). Obviously, the RC time constant is linear with the load resistance ( $R_L$ ) and the ratio is the capacitance ( $C$ ). In order to analyze the mechanism in the decay component of the pulse response, we measured the response time of the photodetector with different load resistances as shown in Fig. 5. As seen, the decay time is linearly dependent on the load resistance due to a good linear fit of the experiment data. Therefore, we believe that pulse response of the  $\text{Mg}_{0.48}\text{Zn}_{0.52}\text{O}$  MSM photodetector is RC time limited, and more details will be needed further.

#### 4. Conclusion

In summary, a single phased cubic  $\text{Mg}_{0.48}\text{Zn}_{0.52}\text{O}$  thin film has been prepared on sapphire substrates by MOCVD, and the MSM structured photodetector fabricated on the film shows a low dark current of 6.5 pA at 10 V bias. A maximum responsivity of 16 mA/W is obtained at 268 nm with cutoff wavelength at 283 nm, corresponding to an external quantum efficiency of 7%. Especially, the rise and decay time of the device is 10 ns and 150 ns, respectively, with a load resistance of 50  $\Omega$ , which is the first response time ever reported in  $\text{MgZnO}$  solar-blind photodetectors. The pulse response of the device is limited by the RC time constant.

#### Acknowledgements

This work is supported by the Key Project of National Natural Science Foundation of China under Grant No. 50532050, the "973" Program under Grant Nos. 2006CB604906 and 2008CB317105, and the Knowledge Innovation Program of the Chinese Academy of Sciences, Grant No. KJ CX3.SYW.W01.

#### References

- [1] M. Razeghi, A. Rogalski, *J. Appl. Phys.* 79 (1996) 7433.
- [2] J.C. Carrano, T. Li, P.A. Grudowski, R.D. Dupuis, J.C. Campbell, *IEEE Circuits Devices Mag.* 15 (1999) 15.
- [3] E. Monroy, III-Nitride-based UV photodetectors, 1st ed., in: M.O. Manasreh (Ed.), *III-V Nitride Semiconductors Applications and Devices*, vol. 16, Taylor & Francis, New York, 2003, p. 525.
- [4] I.H. Lee, *Phys. Stat. Sol. (a)* 192 (2002) R4.
- [5] J.Y. Duboz, J.L. Reverchon, D. Adam, B. Damilano, F. Semond, N. Grandjean, J. Massies, *Phys. Stat. Sol. (a)* 188 (2001) 325.
- [6] N. Biyikli, I. Kimukin, T. Kartaloglu, O. Aytur, E. Ozbay, *Phys. Stat. Sol. (c)* 0 (2003) 2314.
- [7] J.L. Pau, E. Muñoz, M.A. Sánchez, E. Calleja, *Proceedings of SPIE*. 4650 (2002) 104.
- [8] S.V. Averin, P.I. Kuznetsov, V.A. Zhitov, N.V. Alkeev, *Opt Quant Electron.* 39 (2007) 181.
- [9] P. Bhattacharya, *Semiconductor Optoelectronic Devices*, Prentice Hall, Englewood Cliffs, NJ, 1994, p. 395.
- [10] E. Monroy, F. Calle, E. Muñoz, F. Omnes, *Appl. Phys. Lett.* 74 (1999) 3401.
- [11] V.V. Kuryatkov, B.A. Borisov, S.A. Nikishin, *J. Appl. Phys.* 100 (2006) 096104.
- [12] S. Choojun, R.D. Vispute, W. Yang, R.P. Sharma, T. Venkatesan, H. Shen, *Appl. Phys. Lett.* 80 (2002) 1529.
- [13] Z.G. Ju, C.X. Shan, D.Y. Jiang, J.Y. Zhang, B. Yao, D.X. Zhao, D.Z. Shen, X.W. Fan, *Appl. Phys. Lett.* 93 (2008) 173505.
- [14] E.M. Levin, C.R. Robbins, H.F. McMurdie, M.K. Reser, *Phase Diagrams for Ceramicists*, American Ceramic Society, Columbus, Ohio, 1964.
- [15] W. Yang, R.D. Vispute, S. Choojun, R.P. Sharma, T. Venkatesan, *Appl. Phys. Lett.* 78 (2001) 2787.
- [16] K. Kazuto, H. Kenji, N. Ippei, T. Gen-You, O. Ken-Ichi, S. Shigehiko, I. Ma-sataka, Y. Mitsuaki, *J. Crystal Growth*. 278 (2005) 288.
- [17] I. Takeuchi, W. Yang, K.S. Chang, M.A. Aronova, T. Venkatesan, *J. Appl. Phys.* 94 (2003) 7336.
- [18] J.L. Pau, E. Muñoz, M.A. Sánchez, E. Calleja, *Proc. SPIE*. 4650 (2002) 104.
- [19] D. Walker, E. Monroy, P. Kung, J. Wu, M. Hamilton, F.J. Sanchez, J. Diaz, M. Razeghi, *Appl. Phys. Lett.* 74 (1999) 762.
- [20] N. Biyikli, I. Kimukin, T. Tut, O. Aytur, E. Ozbay, *Electronics Letters*. 41 (2005) 274.